Available online at www.sciencedirect.com
SCIENCE DIRECT®
Journal of Organometallic Chemistry 678 (2003) 82–89
Journal of Organometallic Chemistry
www.elsevier.com/locate/jorganchem

Linear ditopic acetylide gold or mercury complexes: synthesis and photophysic studies X-ray crystal structure of $PPh_4[Au(C{\equiv}CC_5H_4N)_2]$

Montserrat Ferrer [a,*], Laura Rodríguez [a], Oriol Rossell [a], Fernando Pina [b], João C. Lima [b], Mercè Font Bardia [c], Xavier Solans [c]

[a] Departament de Química Inorgànica, Universitat de Barcelona, Martí i Franquès 1-11, 08028 Barcelona, Spain
[b] Departamento de Química, Centro de Química Fina e Biotecnologia, Universidade Nova de Lisboa, Quinta de Torre, 2825 Monte da Caparica, Portugal
[c] Departament de Cristal.lografia, Mineralogia i Dipòsits Minerals, Universitat de Barcelona, Martí i Franquès s/n, 08028 Barcelona, Spain

Received 9 April 2003; received in revised form 9 May 2003; accepted 9 May 2003

Abstract

The AlkH alkyne compounds 4-ethynylpyridine (**1**), 4-ethynylbenzonitrile (**2**) and (4-ethynylphenyl)(4-pyridyl)acetylene (**3**) react with $[PPh_4][Au(acac)_2]$ to yield three new linear ditopic bis-alkyne gold(I) compounds $[PPh_4][Au(Alk)_2]$ (for AlkH = **1**, **1a**; for AlkH = **2**, **2a** and for AlkH = **3**, **3a**). The reaction of **1a** with an excess of methyl iodide results in the methylation of both N-pyridine atoms. Analogous mercury(II) $[Hg(Alk)_2]$ compounds are obtained by the reaction of the lithium derivatives of **1**, **3** and (4-bromophenyl)(4-pyridyl)acetylene (**4**) with $HgCl_2$. All these compounds have been characterised by IR and ^{1}H-NMR spectroscopies and mass spectrometry. The X-ray crystal structure of **1a** shows that the gold atom is surrounded by two alkyne ligands in a linear fashion. The reported compounds have been tested as building blocks for the synthesis of molecular polygons by self-assembly. Emission of the compounds was studied and the measured quantum yields were in the range $0.01 < \Phi < 0.04$. Room-temperature emission of compounds **1aH** and **1a′** exhibits a large Stokes shift, and is assigned to the lower triplet state. Decay times were measured at room temperature in CH_2Cl_2 for **1aH** (1.5 μs) and in ethanol at 77 K (149 and 500 μs for compounds **1aH** and **1a′**, respectively). Room-temperature emission of compounds **3a** and **3aH** arises from the lower singlet state and phosphorescence is only observed at 77 K. Theoretical calculations on the nature and energy of singlet and triplet states corroborate the assignments.

Keywords: Photoluminescence; Supramolecular; Acetylide; Gold; Mercury

1. Introduction

Recently, the chemistry of metal acetylides has become the focus of enormous attention with the emerging interest in their potential applications in the field of materials science [1]. In particular, two linear coordinate gold(I) complexes of the type $[AuX_2]^-$ (X = anionic ligand, such as a substituted alkynyl group) have potential as building blocks for supramolecular structures because of their relatively simple molecular geometry. Moreover, for these species there is evidence for ready association into dimers, oligomers and polymers as a result of attractive intermolecular Au···Au interactions [2]. The strengths for the gold–gold interactions are comparable with those found in hydrogen bonds [3] and they seem to be responsible for the intriguing optical properties of some of these species [4]. For example, it has been reported that formation of Au···Au and aryl–aryl interactions in the solid state can lead to the observation of a red-shift in the emission band compared with that in the solution phase [5].

Here we report the synthesis and characterisation of the first linear gold ditopic donor complexes. These species were built of substituted acetylide fragments and

* Corresponding author. Tel.: +34-93-402-12-74; fax: +34-93-490-77-25.
E-mail address: montse.ferrer@qi.ub.es (M. Ferrer).

0022-328X/03/$ - see front matter © 2003 Elsevier Science B.V. All rights reserved.
doi:10.1016/S0022-328X(03)00442-X

were thought to react with ditopic acceptor units such as *cis*-(dppp)M(OTf)$_2$ (M = Pd, Pt) to render molecular polygons. This study has been extended to some analogous mercury compounds. In addition, the photophysical properties of the new species are also discussed.

2. Results and discussion

We aimed to construct supramolecular assemblies resulting from the reaction between metal-containing ditopic donor units with the well-known ditopic acceptor fragments *cis*-(L–L)M(OTf)$_2$ (L–L = bidentate ligand; M = Pd, Pt) [6]. We focused our attention on gold and mercury complexes, given their preference for number of coordination two, which is required for building up molecular polygons such as square or triangular frameworks [7]. We were also interested in using acetylide ligands since they could act as base receptor sites for binding, via the π-tweezer effect, a variety of Lewis acids [8]. On the other hand, the presence of unsaturated bonds in the supramolecular species would permit researchers to carry out photophysics studies on them.

Although a number of acetylide gold complexes have been reported, the vast majority is supported by arylphosphine ancillary ligands [9]. The latter molecules were not suitable for our purposes since they are not able to coordinate simultaneously two metal centres. As a result, we decided to use the ligands **1**, **2**, **3** and **4**, as shown in Scheme 1. These ligands exhibit one coordination site for the metal atom (gold or mercury) while another (arylnitrile or pyridine unit), at 180°, is free for a further coordination.

Compounds **1a**, **2a** and **3a**, which can be formally considered as metal-containing edges, were easily prepared by making [PPh$_4$][Au(acac)$_2$] react with the corresponding terminal alkyne ligand in dichloromethane at room temperature (Scheme 2). Yields were about 70%. Evidence for the proposed structures is seen in the IR spectra, which showed ν(C≡C) bands about 2100 cm^{-1}, shifted to higher frequencies (10–20 cm^{-1}) than that of the starting organic ligand. The ν(C≡N) stretch for **2a** appears at 2229 cm^{-1}. ^{1}H-NMR spectroscopy showed the disappearance of the terminal acetylene proton in **1**, **2** and **3**, and the aromatic protons were unambiguously assigned. The ESMS spectrum of **2a** permitted us to detect the molecular peak at *m*/*z* 448.9, while those corresponding to **1a** (*m*/*z* 401.1) and **3a** (*m*/*z* 601.7) were obtained from FABMS experiments. The geometry of **1a** has been confirmed by an X-ray crystal structure determination.

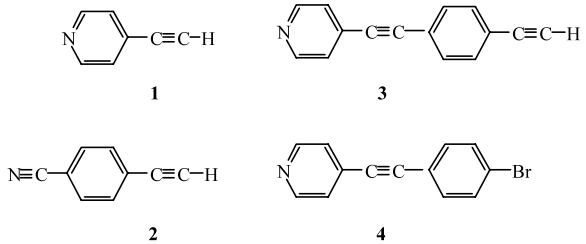

Scheme 1.

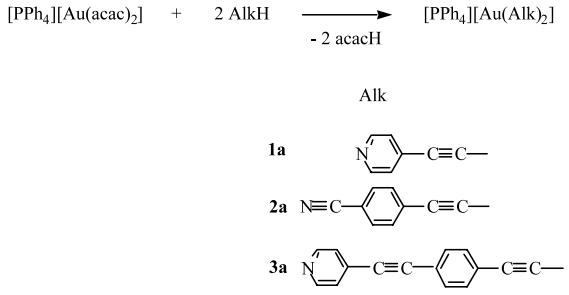

Scheme 2.

In an attempt to obtain a gold(III) derivative starting from **1a**, we made it react with an excess of methyl iodide; however, the isolated compound was the salt **1a**′ (Scheme 3) resulting from methylation of both N-pyridine atoms. The spectroscopic data are close to those found in **1a** and the methyl protons appear at 4.18 ppm in DMSO-d_6.

We have extended this type of compounds to mercury and, thus, the species **1b**, **3b** and **4b** were prepared from **1**, **3** and **4**, respectively (Scheme 4). The synthetic procedure consisted of two steps: the first involved the lithiation with ^{n}BuLi of **1**, **3** or **4** in THF at −78 °C, and the second, the subsequent reaction with $HgCl_2$. Yields were reasonably good. The characterisation was carried out by IR and ^{1}H-NMR spectroscopies and FABMS.

Notably, in **3a** and **3b**, two ν(C≡C) stretches appear, one corresponding to the alkynyl group directly attached to metal (2094 cm^{-1} for **3a** and 2145 cm^{-1} for **3b**, as reported for the majority of mercury-bisalkynyl complexes) and another corresponding to the alkynyl unit unbonded to the metal at 2214 cm^{-1}. This fact suggests that partial electron density from the metal atoms is given up to π* molecular orbitals of the alkynyl groups, this effect being more pronounced for the gold complex because of the smaller positive charge on the metal atom. The FABMS revealed the M+H$^+$ ion

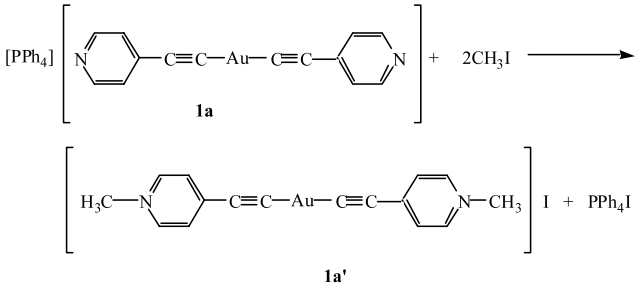

Scheme 3.

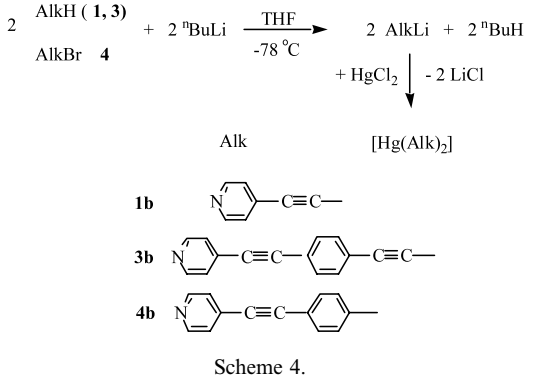

Scheme 4.

Table 1
Selected interatomic distances (Å) and bond angles (°) of **1a**

Au–C(1)	1.980(8)
Au–C(8)	1.983(8)
C(1)–C(2)	1.206(10)
C(8)–C(9)	1.213(10)
C(2)–C(3)	1.420(10)
C(9)–C(10)	1.420(10)
C(1)–Au–C(8)	176.2(2)
C(2)–C(1)–Au	177.0(5)
C(9)–C(8)–Au	173.2(6)
C(8)–C(9)–C(10)	176.1(8)
C(1)–C(2)–C(3)	177.2(7)

peaks at *m*/*z* 405.8, 606.2 and 556.9 for **1b**, **3b** and **4b**, respectively.

In the crystals of **1a**, $[Au(C{\equiv}CC_5H_4N)_2]^-$ anions and PPh_4^+ cations are present. The structure of the gold compound is shown in Fig. 1; selected bond and angle parameters are listed in Table 1. As expected, the geometry about the gold(I) centre is linear with C(1)–Au–C(8) angle of 176.2(2)° and the angles C(3)–C(2)–C(1) and C(8)–C(9)–C(10) = 177.2(7)° and 176.1(8)°, respectively, close to the ideal value of 180° for a rigid-rod molecule. The gold–carbon distances, Au–C(1) (1.980(8) Å) and Au–C(8) (1.983(8) Å), as well as the triple bond distances, C(1)–C(2) (1.206(10) Å) and C(8)–C(9) (1.213(10) Å), are similar to those in related acetylide complexes [5a,10]. In contrast to most Au(I) compounds, where there exist short Au···Au intermolecular contacts, no such short interactions are observed in **1a** (Au···Au = 5.46 Å) as the negative charge on it probably prevents their close approach.

2.1. Attempts to obtain molecular polygons

It is well-known that the stoichiometric combination of 90° corners with linear linking units can lead to square or triangular entities. Although a great number of "organic" edges have been employed, only a small number of metal-containing edges are known [11]. The synthesis of **1**–**3a** and **1b**, **3b** and **4b** allowed us to test them as gold- or mercury-linkers towards the ditopic acceptor units (diphosphine)$M(OTf)_2$ (M = Pd, Pt). In most cases, only intractable insoluble materials were obtained that did not allowed the growing of single crystals suitable for a structure determination. On the other hand, when no precipitate was obtained, ^{31}P- and ^1H-NMR spectra of the reaction solutions showed very complex patterns that could not be assigned. Changes in the reaction conditions, involving variations on the solution concentration (work at high dilution), temperature and solvent (common organic solvents, DMSO, nitromethane, etc.) were performed. However, in no case we were able to modify the nature of the resulting products. These results contrast with those obtained by employing platinum or palladium corners with a wide variety of "organic" edges [7], where square or triangular entities are isolated in reasonable yields and structurally characterised. It is currently unclear why the presence of gold or mercury atoms in the backbone of the edges prevents the formation of the molecular polygons.

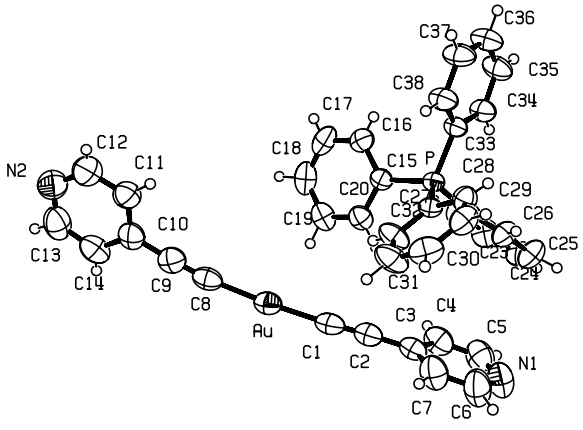

Fig. 1. ORTEP drawing of the molecular structure and numbering scheme of **1a**.

2.2. Photoluminescence studies

The absorption and the luminescence of compounds **1a**, **1a′** and **3a** were carried out in dichloromethane at room temperature. In the case of compound **1a**, the emission only appears in acidic medium (formation of compound **1aH** takes place upon addition of trifluoroacetic acid), while in compound **3a** the emission changes upon acidification, with an increase of the emission quantum yield and a red-shift in the emission band. In the case of compound **2a**, metal ligand dissociation takes place in acidic media, and thus the observed emission is due to the free **2** and protonated ligand. For compounds **1a** and **3a**, the stability of their protonated forms **1aH** and **3aH** was checked by ^1H-NMR.

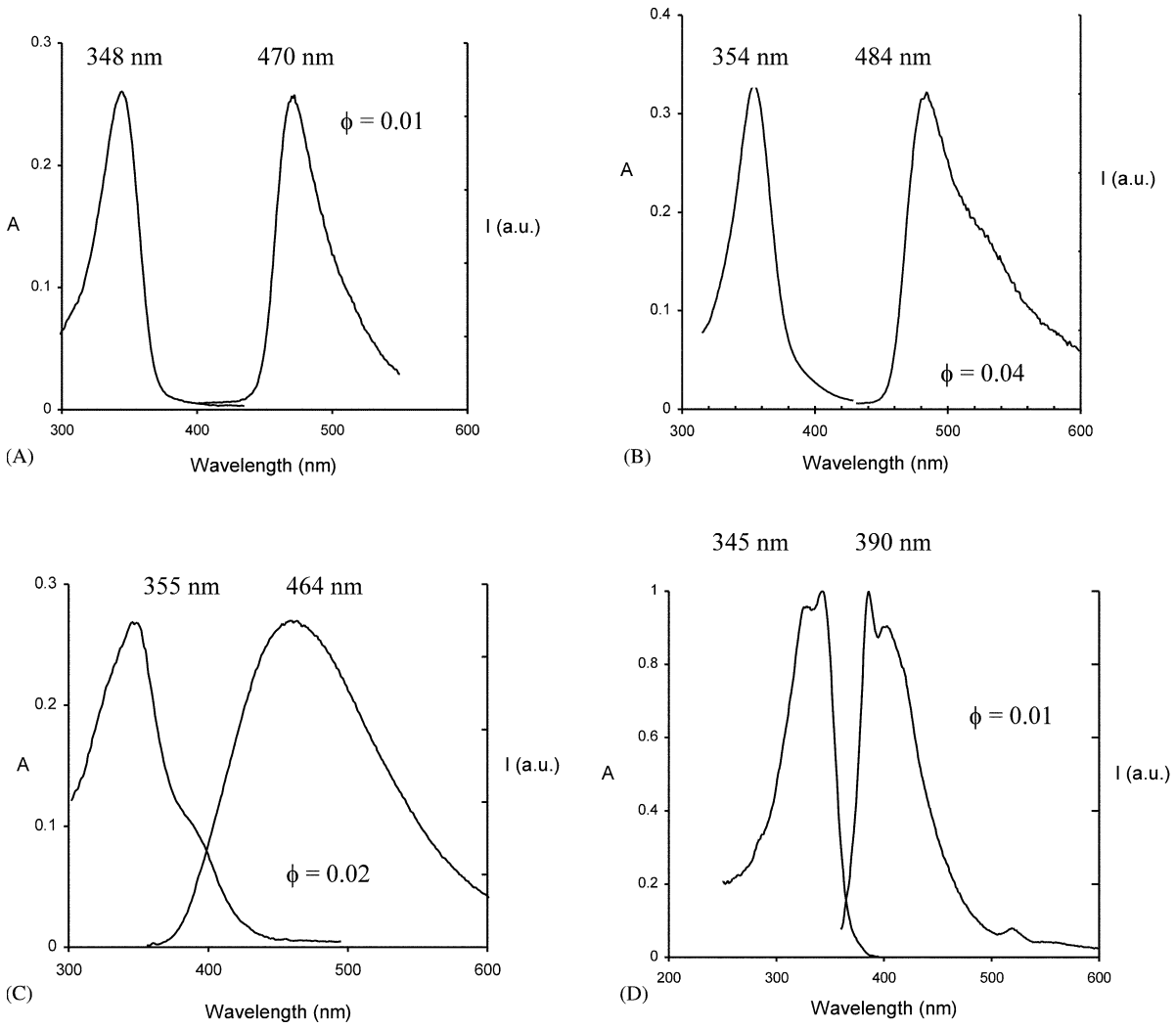

Fig. 2. Absorption and emission spectra of compounds **1aH** (A), **1a**′ (B), **3aH** (C) and **3a** (D).

The absorption and emission of compound **1aH** are reported in Fig. 2A. The absorption spectrum shows a band with shape and intensity similar to the free ligand **1**, and its very high molar absorption coefficient points to an allowed π–π* transition. Similar observations were reported for other compounds containing the Au–C≡C–Ph moiety [12].

A common feature of compounds **1aH** and **1a**′ (see Fig. 2) is a large Stokes shift, suggesting that the emission is not from the same state populated by direct light absorption. Other authors have proposed a triplet as the emissive state for similar gold(I) complexes [13].

In order to understand the origin of the observed transitions in both complexed and uncomplexed forms, state diagrams for the free ligands **1**, **1H**, **1CH$_3$**, **3** and **3H** were obtained using ZINDO/S semi-empirical program (Fig. 3). The same calculations could not be performed in the case of the gold complexes, since the semi-empirical parameters for the metal atom are not available. Fortunately this is not a problem in the particular case of the compounds under study, since absorption spectra of the free and complexed forms are identical and new transitions arising from metal complexation were not observed.

According to the state diagrams, both protonated and unprotonated forms of ligand **1** exhibit forbidden low-lying singlet excited states, as is predicted for the case of the ligand **1CH$_3$**. In the case of ligand **1**, the low-lying singlet (S_1) is $n\pi^*$ in nature, while in **1H** and **1CH$_3$**, S_1 is $\pi_{xy}\pi^*$. The $\pi_{xy}\pi^*$ state arises from the transition of one electron from a π molecular orbital localised in the triple bond that is perpendicular to the conjugated π system to an antibonding orbital of the π conjugated system. It is, thus, a forbidden transition. These predictions are

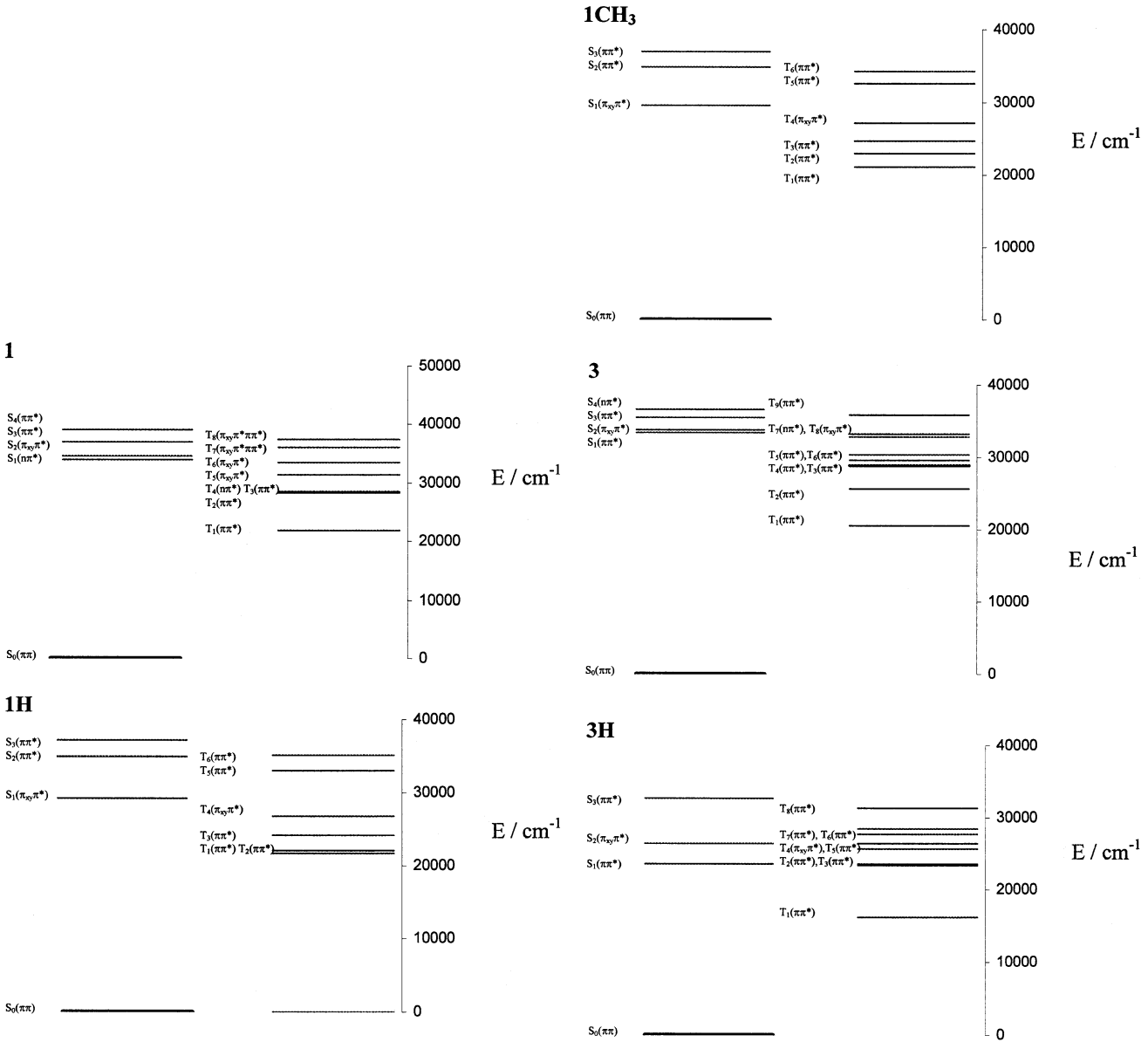

Fig. 3. State diagrams for compounds **1**, **1H**, **1CH$_3$**, **3** and **3H**.

compatible with the experimental observation that the free ligand **1** does not emit in either protonated or unprotonated form.

Upon metal complexation, **1aH** and **1a′** show a strongly red-shifted emission, which arises from the low-lying triplet state T_1, $\pi\pi^*$ in nature, populated through the enhanced intersystem crossing due to heavy atom effect. Compound **1a** does not emit, and the reason for that behaviour is not fully understood.

The phosphorescence quantum yield of **1aH** is $\Phi = 0.01$. The decay time measured by laser flash photolysis at room temperature in dichloromethane/trifluoroacetic acid is 1.5 μs and in low-temperature rigid media (ethanol at 77 K) is 149 μs, confirming that this emission is of triplet origin.

Concerning the analogous to **1a** but containing mercury instead of gold (compound **1b**), no emission was detected in neutral or acidic media.

The absorption and emission of compound **1a′** exhibit an identical pattern to **1aH**, as could be predicted by the very close state diagrams of the ligands of both compounds. In **1a′**, both bands are slightly red-shifted (Fig. 2B) due to the methyl substituent as found in other similar compounds [14]. In rigid media at low temperature (ethanol at 77 K), the triplet of compound **1a′** has a longer lifetime (500 μs) than the triplet of **1aH** in the same conditions (149 μs).

Room-temperature solid-state luminescence spectrum, i.e., luminescence of the powder, was collected for compound **1a′** and is shown in Fig. 4, together with

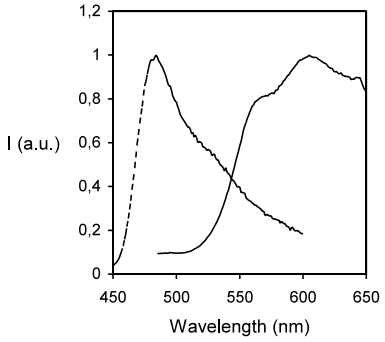

Fig. 4. Solution (dashed line) and solid (solid line) emission spectra of compound **1a**′.

the emission spectrum collected in solution. The emission of the powder is strongly red-shifted and presents a shape that is completely different from what is observed in solution, suggesting a strong interaction between the monomers and extended π–π interactions.

The state diagram for ligand **3**, presents a low-lying ππ* singlet state in both protonated and unprotonated forms. This is in good agreement with the observation of fluorescence emission for both forms, being the emission of the protonated form (450 nm) red-shifted with respect to the unprotonated (328 nm) and presenting a higher fluorescence quantum yield. Complexation induces small shifts in the emission but does not induce the appearance of a new phosphorescence band at room temperature such as the observed with the previous compounds. The absorption and emission spectra of compound **3aH** are presented in Fig. 2C. The shoulder observed in the absorption spectrum of compound **3aH** could be due to the lower energy singlet (ca. 400 nm), predicted by the state diagram, whose low energy can be explained by increasing conjugation in the π system of this compound. The luminescence is broader and blue-shifted in comparison with compounds **1aH** and **1a**′. The Stokes shift is now much smaller and its singlet assignment is straightforward. Time-correlated single photon counting was used to measure the fluorescence decay of compound **3aH**. The decays collected at several emission wavelengths are always best-fitted with a sum of two exponentials whose origin is still unclear. Despite the attribution of other authors of similar bi-exponential behaviour to the presence of monomers and excimers, we have no evidence for excimer formation in this case [15]. The average decay time measured is 2.2 ns.

Despite the fact that fluorescence is rarely observed in the case of transition metal complexes, it is clearly observed for compounds **3a** and **3aH**. The radiative rate constant of the low-lying (strongly allowed) ππ* state competes in magnitude with the intersystem crossing rate constant, even after complexation with the metal [16]. However, complexation does affect the fluorescence quantum yield, i.e., the complexed form (**3aH**; $\Phi = 0.02$) has a lower quantum yield than the free ligand (**3H**; $\Phi = 0.08$). This is a result of the increase in the intersystem crossing due to the heavy atom effect. In this case, the increase of intersystem crossing is not accompanied by the appearance of room-temperature phosphorescence. The reason for that is probably the fact that the triplet is so low in energy that coupling with the ground state leads to a very efficient non-radiative deactivation pathway of the triplet. In rigid media, at low temperature (ethanol at 77 K), the non-radiative constant becomes significantly less important and phosphorescence is clearly observed (decay time = 670 μs).

3. Experimental

All manipulations were performed under prepurified N_2 using standard Schlenk techniques. All solvents were distilled from appropriate drying agents. Infrared spectra were recorded on an FT-IR 520 Nicolet spectrophotometer. $^{31}P\{^1H\}$-NMR (δ (85% H_3PO_4) = 0.0 ppm) and ^1H-NMR spectra were obtained on a Bruker DXR 250 and Varian 200 spectrometers. Elemental analyses of C, H and N were carried out at the Institut de Bio-Orgànica in Barcelona. FABMS and electrospray mass spectra were recorded on a Fisons VG Quattro spectrometer. Absorption spectra were recorded in a Perkin–Elmer Lambda 6 spectrophotometer, and fluorescence emission on a SPEX F111 Fluorolog spectrofluorimeter. Total luminescence quantum yields were measured relatively to quinine sulphate in 1 N H_2SO_4, $\Phi = 0.54$. Luminescence decays were obtained with an applied photophysics laser flash photolysis equipment pumped by an Nd:YAG laser (Spectra Physics) with excitation at 355 nm [17] and a SPEX Fluorolog F2121, with excitation at 355 nm. The emission mode was used to obtain the luminescence decays. Compounds 4-ethynylpyridine [18], 4-ethynylbenzonitrile [19], (4-bromophenyl)(4-pyridyl)acetylene [20], (4-ethynylphenyl)(4-pyridyl)acetylene [20] and $[PPh_4][Au(acac)_2]$ [21] were prepared as described previously.

Energy of the states were obtained performing single point calculations with ZINDO/S-CI (99 singly excited configurations) on geometries optimised with PM3. Both semi-empirical programs used belong to the package Hyperchem™, release 6.01 for Windows, Copyright© 2000 Hypercube, Inc.

3.1. Synthesis of $[PPh_4][Au(C{\equiv}CC_5H_4N)_2]$ (**1a**)

Solid 4-ethynylpyridine (**1**) (0.17 g, 1.64 mmol) was added to a CH_2Cl_2 (40 ml) solution of $[PPh_4][Au(acac)_2]$ (0.3 g, 0.41 mmol) at room temperature. After 30 min of stirring, the reaction mixture was filtered through Celite, concentrated to 5 ml under vacuum and diethylether was added (20 ml). During all the manipulations, the solution was protected from the light in order to avoid

decomposition. A pale pink solid was obtained in 70% yield. IR (KBr, cm^{-1}), ν(C≡C): 2106. ^{1}H-NMR (298 K, acetone-d_6, δ ppm): 7.11 (d, $J_{H-H} = 5.9$ Hz, 4H, $H_{\beta\text{-pyr}}$), 7.56–7.92 (m, 20H, PPh_4^+), 8.33 (d, $J_{H-H} = 5.9$ Hz, 4H, $H_{\alpha\text{-pyr}}$). FABMS [M^-]; *m/z*: Calc.: 401.0; Found: 401.1. Anal. Calc.: C, 61.59; H, 3.80; N, 3.80. Found: C, 61.61; H, 3.84; N, 3.82%.

3.2. Syntheses of $[PPh_4][Au(C{\equiv}CC_6H_4CN)_2]$ (**2a**) and $[PPh_4][Au(C{\equiv}CC_6H_4C{\equiv}CC_5H_4N)_2]$ (**3a**)

Details of synthesis of **1a** also apply to **2a** and **3a**.

2a: IR (KBr, cm^{-1}), ν(C≡N): 2229, ν(C≡C): 2106. ^{1}H-NMR (298 K, $CDCl_3$, δ ppm): 7.22 (m, 4H, H_m), 7.34–7.45 (m, 20H, PPh_4^+), 7.63 (m, 4H, H_o). ESMS [M^-]; *m/z*: Calc.: 448.9; Found: 448.9. Anal. Calc.: C, 63.93; H, 3.55; N, 3.52. Found: C, 63.97; H, 3.60; N, 3.57%.

3a: IR (KBr, cm^{-1}), ν(C≡C): 2214 ($NC_5H_4C{\equiv}C$), 2094 ($C{\equiv}C$Au). ^{1}H-NMR (298 K, acetone-d_6, δ ppm): 7.27 (m, 4H, H_m, AA′XX′ spin system), 7.38 (m, 4H, H_o, AA′XX′ spin system), 7.44 (dd, 4H, $H_{\beta\text{-pyr}}$, AA′XX′ spin system), 7.84–8.04 (m, 20H, PPh_4^+), 8.58 (dd, 4H, $H_{\alpha\text{-pyr}}$, AA′XX′ spin system). FABMS [M^-]; *m/z* Calc.: 601.0; Found: 601.7. Anal. Calc.: C, 68.91; H, 3.82; N, 2.98. Found: C, 68.95; H, 3.88; N, 2.99%.

3.3. Synthesis of $[Au(C{\equiv}CC_5H_4NCH_3)_2]I$ (**1a′**)

CH_3I (0.12 ml, 1.9 mmol) was added dropwise to an acetone (15 ml) solution of **1a** (0.14 g, 0.19 mmol) at room temperature. After 45 min of stirring, a yellow solid was obtained in 65% yield. IR (KBr, cm^{-1}), ν(C≡C): 2109. ^{1}H-NMR (298 K, DMSO-d_6, δ ppm): 4.18 (s, 6H, CH_3), 7.79 (d, $J_{H-H} = 6.5$ Hz, 4H, $H_{\beta\text{-pyr}}$), 8.68 (d, $J_{H-H} = 6.5$ Hz, 4H, $H_{\alpha\text{-pyr}}$). FABMS [M^+]; *m/z* Calc.: 431.0; Found: 431.6. Anal. Calc.: C, 86.04; H, 6.09; N, 5.02. Found: C, 86.08; H, 6.12; N, 5.08%.

3.4. Synthesis of $[Hg(C{\equiv}CC_5H_4N)_2]$ (**1b**)

To a precooled (−78 °C) solution of 4-ethynylpyridine (**1**) (0.11 g, 1.11 mmol) in THF (20 ml) was added dropwise ^{n}BuLi (0.10 ml, 1.11 mmol). The solution turned pale yellow immediately. After 30 min of stirring, solid $HgCl_2$ (0.10 g, 0.37 mmol) was added. The mixture was stirred for 1 h at room temperature and then concentrated to 5 ml. A white solid was obtained after the addition of ethanol (20 ml) in 62% yield. IR (KBr, cm^{-1}), ν(C≡C): 2150. ^{1}H-NMR (298 K, $CDCl_3$, δ ppm): 7.33 (d, $J_{H-H} = 11.9$ Hz, 4H, $H_{\beta\text{-pyr}}$), 8.58 (d, $J_{H-H} = 11.9$ Hz, 4H, $H_{\alpha\text{-pyr}}$). FABMS [$M+H^+$]; *m/z* Calc.: 405.6; Found: 405.8. Anal. Calc.: C, 41.52; H, 1.98; N, 6.92. Found: C, 41.55; H, 2.01; N, 6.97%.

3.5. Syntheses of $[Hg(C{\equiv}CC_6H_4C{\equiv}CC_5H_4N)_2]$ (**3b**) and $[Hg(C_6H_4C{\equiv}CC_5H_4N)_2]$ (**4b**)

Details of synthesis of **1b** also apply to **3b** and **4b**.

3b: IR (KBr, cm^{-1}) ν(C≡C): 2214 ($NC_5H_4C{\equiv}C$), 2145 ($C{\equiv}C$Hg). ^{1}H-NMR (298 K, $CDCl_3$, δ ppm): 7.37 (d, $J_{H-H} = 5.7$ Hz, 4H, $H_{\beta\text{-pyr}}$), 7.49 (s, br, 8H, C_6H_4), 8.61 (d, $J_{H-H} = 5.7$ Hz, 4H, $H_{\alpha\text{-pyr}}$), FABMS [$M+H^+$]; *m/z* Calc.: 605.6; Found: 606.2. Anal. Calc.: C, 59.54; H, 2.65; N, 4.63. Found: C, 59.57; H, 2.69; N, 4.67%.

4b: IR (KBr, cm^{-1}) ν(C≡C): 2214. ^{1}H-NMR (298 K, DMSO-d_6, δ ppm): 7.40 (s, br, 8H, C_6H_4), 7.52 (s, 4H, $H_{\beta\text{-pyr}}$), 8.48 (s, 4H, $H_{\alpha\text{-pyr}}$). FABMS [$M+H^+$]; *m/z* Calc.: 557.5; Found: 556.9. Anal. Calc.: C, 56.05; H, 2.87; N, 5.03. Found: C, 56.07; H, 2.90; N, 5.06%.

3.6. X-ray structure determination of **1a**

A prismatic crystal ($0.1 \times 0.1 \times 0.2$ mm^3) was selected and mounted on a MAR345 diffractometer with an image plate detector. Unit cell parameters were determined from automatic centring of 8588 reflections ($3° < \theta < 31°$) and refined by least-squares method. Intensities were collected with graphite monochromatised Mo–K_α radiation. 11 197 reflections were measured in the range $1.70° \leq \theta \leq 28.82°$. 6435 of which were non-equivalent by symmetry (R_{int} (on I) = 0.023). 5373 reflections were assumed as observed applying the condition $I > 2\sigma(I)$. Lorentz polarisation and absorption corrections were made. Numerical details have been collected in Table 2.

The structure was solved by direct methods, using SHELXS computer program [22] and refined by the full-matrix least-squares method with the SHELX93 computer program [23] using 6435 reflections (very negative intensities were not assumed). The function minimised was $\Sigma w||F_o|^2-|F_c|^2|^2$, where $w = [\sigma^2(I)+(0.0607P)^2 +2.4230P]^{-1}$, and $P = (|F_o|^2+2|F_c|^2)/3$, f, f' and f'' were taken from International Tables of X-ray Crystallography [24]. 22H atoms were located from a difference synthesis and refined with an overall isotropic temperature factor. 6H atoms were computed and refined, using a riding model, with an isotropic temperature factor equal to 1.2 times the equivalent temperature factor of the atom which is linked.

4. Supplementary material

Crystallographic data for the structural analysis have been deposited with the Cambridge Crystallographic Data Centre, CCDC No. 200097 for compound **1a**. Copies of this information may be obtained free of charge from The Director, CCDC, 12 Union Road, Cambridge CB2 1EZ, UK (Fax: +44-1223-336033; e-mail: deposit@ccdc.cam.ac.uk or http://www.ccdc.cam.ac.uk).

Table 2
Crystal data and details of the structure determination of **1a**

Empirical formula	$C_{38}H_{28}AuN_2P$
Formula weight	740.56
Temperature (K)	293(2)
Wavelength (Å)	0.71069
Crystal system	triclinic
Space group	$P\bar{1}$
Unit cell dimensions	
a (Å)	10.8070(10)
b (Å)	12.7260(10)
c (Å)	13.8840(10)
α (°)	106.260(10)
β (°)	107.717 (10)
γ (°)	109.210 (10)
V (Å^3)	1556.6(2)
Z	2
D_{calc} (mg m^{-3})	1.580
Absorption coefficient (mm^{-1})	4.806
$F(0\ 0\ 0)$	728
Crystal size (mm^3)	$0.1 \times 0.1 \times 0.2$
Theta range for data collection (°)	1.70–28.82
Index ranges	$0 \le h \le 14$, $-17 \le k \le 16$, $-18 \le l \le 17$
Reflections collected/unique	11 197/6435 [$R_{int} = 0.0234$]
Refinement method	Full-matrix least-squares on F^2
Data/restraints/parameters	6435/0/467
Goodness-of-fit on F^2	1.131
Final R indices [$I > 2\sigma(I)$]	$R_1 = 0.0401$, $wR_2 = 0.1040$
R indices (all data)	$R_1 = 0.0549$, $wR_2 = 0.1209$
Largest difference peak and hole (e Å^{-3})	0.790 and −0.624

Acknowledgements

This work was supported by the DGICYT (Project BQU2000-0644) and the CIRIT (Project 1999 SGR 00045). L.R. is indebted to the Universitat de Barcelona for a scholarship. We are indebted to Prof. J.S. de Melo from Departamento de Química, Faculdade de Ciências e Tecnologia, of the Universidade de Coimbra for lifetime measurements.

References

[1] (a) L. Ouahab, Chem. Mater. 9 (1997) 1909 (and references therein);
(b) D.M. Mingos, R. Vilar, D. Raia, J. Organomet. Chem. 641 (2002) 126.
[2] (a) H. Schmidbaur, Gold. Bull. 23 (1990) 11;
(b) H. Schmidbaur, Chem. Soc. Rev. 24 (1995) 391;
(c) P. Pyykkö, Chem. Rev. 97 (1997) 597.
[3] (a) B.C. Tzeng, A. Schier, H. Schmidbaur, Inorg. Chem. 38 (1999) 3978;
(b) C. Hollatz, A. Schier, H. Schmidbaur, J. Am. Chem. Soc. 119 (1997) 8115.
[4] C. King, J.C. Wang, M.N.I. Kham, J.P. Fackler, Jr., Inorg. Chem. 28 (1989) 2145.
[5] (a) M.J. Irwin, J.J. Vittal, R.J. Puddephatt, Organometallics 16 (1997) 3541;
(b) V.W.W. Yam, K.K.W. Lo, Chem. Soc. Rev. 28 (1999) 323;
(c) W.J. Hunks, M.A. MacDonals, M.C. Jennings, R.J. Puddephatt, Organometallics 19 (2000) 5063.
[6] P.J. Stang, D.H. Cao, J. Am. Chem. Soc. 116 (1994) 4981.
[7] (a) P.J. Stang, Chem. Eur. J. 4 (1998) 19;
(b) M. Fujita, Chem. Soc. Rev. 27 (1998) 417.
[8] (a) J. Manna, C.J. Kuehl, J.A. Whiteford, P.J. Stang, D.C. Muddiman, S.A. Hofstadler, R.D. Smith, J. Am. Chem. Soc. 119 (1997) 11611;
(b) J.A. Whiteford, P.J. Stang, S.D. Huang, Inorg. Chem. 37 (1998) 5595.
[9] A. Grohmann, H. Schmidbaur, in: E.W. Abel, F.G.A. Stone, G. Wilkinson (Eds.), Comprehensive Organometallic Chemistry, vol. 3, Pergamon Press, Oxford, 1995, pp. 1–56.
[10] (a) B.C. Tzeng, W.C. Lo, C.M. Che, S.M. Peng, Chem. Commun. (1996) 181.;
(b) C.M. Che, H.K. Yip, W.C. Lo, S.M. Peng, Polyhedron 13 (1994) 887;
(c) W. Lu, H.F. Xiang, N. Zhu, C.M. Che, Organometallics 21 (2002) 2343;
(d) C.M. Che, H.Y. Chao, V.M. Miskowski, Y. Li, K.K. Cheung, J. Am. Chem. Soc. 123 (2001) 4985;

See, for example
[11] (a) B. Olenyyuk, A. Fechtenkötter, P.J. Stang, J. Chem. Soc. Dalton Trans. (1998) 1707.;
(b) S.-S. Sun, A.J. Lees, Inorg. Chem. 40 (2001) 3154.
[12] V.W.-W. Yam, K.K.-W. Lo, K.M.-C. Wong, J. Organomet. Chem. 578 (1999) 3.
[13] H. Xiao, K.-K. Cheung, C.M. Che, J. Chem. Soc. Dalton Trans. (1996) 3699.
[14] E.C. Constable, A.M.W. Cargill Thompson, J. Chem. Soc. Dalton Trans. (1994) 1409.
[15] S.-S. Sun, A.J. Lees, Coord. Chem. Rev. 230 (2002) 171.
[16] A.J. Lees, Chem. Rev. 87 (1987) 711.
[17] J.S. de Melo, L.M. Silva, M. Kuroda, J. Chem. Phys. 115 (2001) 5625.
[18] L.D. Ciana, A. Haim, J. Heterocycl. Chem. 21 (1984) 607.
[19] S. Takahashi, Y. Kuroyama, K. Sonogashira, N. Hagihara, Synthesis (1980) 627 (we have used $Pd(PPh_3)_4$ as a catalyst instead of $[PdCl_2(PPh_3)_2]$).
[20] I.-Y. Wu, J.T. Lin, J. Luo, S.-S. Sun, C.-S. Li, K.-J. Lin, C. Tsai, C.-C. Hsu, J.-L. Lin, Organometallics 16 (1997) 2038.
[21] J. Vicente, M.T. Chicote, Inorg. Synth. 32 (1998) 172.
[22] G.M. Sheldrick, Acta Crystallogr. Sect. A 46 (1990) 467.
[23] G.M. Sheldrick, A Computer Program for Determination of Crystal Structures, University of Göttingen, Germany, 1994.
[24] International Tables of X-ray Crystallography, Vol. IV, Kynoch, Birmingham, 1974, pp. 99–100, 149.